Journal of Autoimmunity 123 (2021) 102709

Contents lists available at ScienceDirect

Journal of Autoimmunity

journal homepage: www.elsevier.com/locate/jautimm

Individual functions of the histone acetyl transferases CBP and p300 in regulating the inflammatory response of synovial fibroblasts

Monika Krošel [a,b,c,1], Marcel Gabathuler [a,1], Malgorzata Maciukiewicz [a], Larissa Moser [a], Gideon Isaac Lee [a], Miriam Marks [d], Matija Tomšič [b,c], Oliver Distler [a], Caroline Ospelt [a], Kerstin Klein [a,e,f,*]

[a] Center of Experimental Rheumatology, Department of Rheumatology, University Hospital Zurich, University of Zurich, Switzerland
[b] Department of Rheumatology, University Medical Centre Ljubljana, Ljubljana, Slovenia
[c] Faculty of Medicine, University of Ljubljana, Ljubljana, Slovenia
[d] Schulthess Klinik, Zurich, Switzerland
[e] Department of BioMedical Research, University of Bern, Bern, Switzerland
[f] Department of Rheumatology and Immunology, University Hospital Bern, Bern, Switzerland

ARTICLE INFO

Keywords:
Synovial fibroblast
Histone acetylation
Bromo domain

ABSTRACT

Chromatin remodeling, and a persistent histone 3 lysine 27 acetylation (H3K27ac) in particular, are associated with a sustained inflammatory response of synovial fibroblasts (SF) in rheumatoid arthritis (RA). Here we investigated individual functions of the writers of H3K27ac marks, the homologues histone acetyl transferases (HAT) CBP and p300, in controlling the constitutive and inflammatory gene expression in RA SF. We applied a silencing strategy, followed by RNA-sequencing and pathway analysis, complemented with the treatment of SF with inhibitors targeting the HAT (C646) or bromo domains (I-CBP) of CBP and p300. We showed that CBP and p300 undertook overlapping and, in particular at gene levels, distinct regulatory functions in SF. p300 is the major HAT for H3K27ac in SF and regulated more diverse pathways than CBP. Whereas both factors regulated genes associated with extracellular matrix remodeling, adhesion and proliferation, p300 specifically controlled developmental genes associated with limb development. Silencing of CBP specifically down regulated the TNF-induced expression of interferon-signature genes. In contrast, silencing of p300 resulted in anti- and pro-inflammatory effects. Integration of data sets derived from RNA-sequencing and chromatin immunoprecipitation sequencing for H3K27ac revealed that changes in gene expression after CBP or p300 silencing could be only partially explained by changes in levels of H3K27ac. Inhibition of CBP/p300 using HAT and bromo domain inhibitors strongly mirrored effects obtained by silencing of p300, including anti- and pro-inflammatory effects, indicating that such inhibitors are not sufficient to be used as anti-inflammatory drugs.

1. Introduction

RA is one of the most prominent chronic, inflammatory joint disease, causing cartilage and bone damage [1]. Intrinsically activated synovial fibroblasts (SF) are a key cell population that contributes to RA pathogenesis [2]. Functional studies *in vivo* have demonstrated that RA SF invade into and destroy cartilage [3] and suggested that they are capable to transmigrate into the vasculature and thus spread RA to multiple joints [4]. Recent work has demonstrated that functionally distinct SF subtypes drive cartilage breakdown and promote the persistent inflammation in RA [5,6]. We and others have previously shown that the exposure to pro-inflammatory factors induces a sustained and prolonged inflammatory response in SF [7,8]. Chromatin remodeling, and in particular persistent histone 3 lysine 27 acetylation (H3K27ac), were shown to be associated with the sustained TNF-induced gene expression in RA SF [8]. The presence of H3K27ac marks is a hallmark of active

* Corresponding author. Freiburgstrasse 16p, H5/ H018, CH-3010, Bern, Switzerland.
E-mail addresses: monika.krosel@kclj.si (M. Krošel), marcel.gaba@gmail.com (M. Gabathuler), malgorzataanna.maciukiewicz@usz.ch (M. Maciukiewicz), Larissa.moser@usz.ch (L. Moser), leegideo@msu.edu (G.I. Lee), miriam.marks@kws.ch (M. Marks), matija.tomsic@guest.arnes.si (M. Tomšič), oliver.distler@usz.ch (O. Distler), caroline.ospelt@usz.ch (C. Ospelt), kerstin.klein@dbmr.unibe.ch (K. Klein).
[1] These authors contributed equally.

https://doi.org/10.1016/j.jaut.2021.102709
Received 21 May 2021; Received in revised form 14 July 2021; Accepted 14 July 2021
Available online 23 July 2021

enhancers and is additionally found in gene promoters [9]. Enhancers underlie cell-type- and stimulus-specific cell responses and can activate gene expression at great distances [10,11].

CREB-binding protein (CBP) and p300 constitute a unique group of histone acetyl transferases (HAT) that account for writing H3K27ac marks [12]. Binding of p300 to chromatin regions has been used as a surrogate for H3K27ac to predict the tissue-specific activity of enhancers [13]. However, the recruitment of CBP and p300 to chromatin regions only partially correlates with transcriptional activation and strongly depends on the genomic context [14], indicating that chromatin immunoprecipitation with sequencing (ChIPseq) is not sufficient to identify individual target genes of CBP and p300.

CBP and p300 are multi-domain proteins that serve as co-factors for a wide spectrum of transcription factors and act as scaffolds for large protein complexes that regulate transcription [15]. They exhibit in addition to the HAT "writer" domain, a bromo domain as a "reader" of acetylated lysine residues, and E3 and E4 ligase activities for protein ubiquitination [15,16]. Inhibitors targeting the bromo domains of CBP and p300 are in drug development for malignant and inflammatory diseases [17].

Given their high degree of sequence homology, CBP and p300 are widely considered to have redundant functions (often referred as CBP/p300). Studies in knockout mice have suggested some degree of functional redundancy of the two enzymes but have additionally pointed to the existence of unique functions [15]. Only few studies addressed such enzyme-specific functions and have identified individual targets of CBP and p300 [18,19].

In the present study, our aim was to study individual functions of CBP and p300 and their functional domains in SF. We chose a silencing approach, complemented with inhibitor experiments targeting the HAT and bromo domains of CBP/p300. This enabled us to study the impact of different functional domains on the regulation of gene expression and to address the potential of CBP/p300 bromo domain inhibitors as anti-inflammatory drugs.

2. Material and methods

2.1. Patient samples and cell preparation

Synovial tissues were derived from hand, shoulder and knee joints of RA patients undergoing joint replacement surgery at the Schulthess Clinic Zurich, Switzerland. All patients fulfilled the criteria for the classification of RA [20] or osteoarthritis (OA) [21]. The study was approved by the ethics committee of the Canton of Zurich, Switzerland. Informed consent was obtained from all patients prior the inclusion into the study. SF were isolated and cultured as described elsewhere [22] and used between passages four and eight for all experiments. The characteristics of patients for the cultivation of SF are shown in Table 1.

Table 1
Characteristics of patients.

	RA (n = 25)	OA (n = 5)
age (years, mean (range))	63 (45–82)	69 (53–81)
sex (female/male)	23/2	4/1
disease duration (years, mean (range))	19 (2–36)	ND
RF (positive/negative)	18/3; ND 4	ND
smoker/non-smoker	2/21; ND 2	0/5
medication	ND 1	ND
DMARDs	14	
NSAIDs steroids	2	
biologics	10	
none	10	
	1	
joints	13	3
hand	9	1
shoulder	1	1
knee		

ND not determined, *DMARDs* disease modifying anti-rheumatic drugs, *NSAIDs* nonsteroidal anti-inflammatory drugs.

2.2. Silencing of CBP and p300

1.5×10^5 SF were transfected with antisense LNA gapmeRs (12.5 nM) targeting CBP, p300 or gapmeR control (Qiagen) using lipofectamine (Thermo Scientific). Twenty-four hours after transfection, cells were stimulated with TNF (10 ng/ml) for another 24 h. Supernatants were collected for ELISA and cells were harvested for RNA isolation or Western blotting. Knockdown of CBP and p300 was verified by real-time PCR and Western blotting.

2.3. Treatment of SF with inhibitors

SF were treated with 1 μM of the HAT inhibitor C646 or 1 μM of the bromodomain inhibitor I-CBP 112 (Tocris Bioscience) in absence and presence of TNF (10 ng/ml) for 24 h. Control SF were treated with matched amounts of dimethylsulfoxid. Cells (n = 6) were harvested 24 h after treatment.

2.4. Real-time PCR

Total RNA was isolated using the RNeasy Mini Kit (Qiagen) and was reversed transcribed [23]. Real-time PCR (7900HT real-time PCR system, Life Technologies) was performed using self-designed primers (Microsynth, supplementary table 1) and SYBR green (Roche). Dissociation curves and samples containing the untranscribed RNA were measured in parallel. Constitutively expressed human ribosomal protein large P0 (RPLP0) was measured for internal standard sample normalization and relative mRNA expression levels were calculated by the comparative threshold cycle method (ΔΔCt) [24].

2.5. Western blotting

Cells were lysed in Laemmli buffer (62.5 mM TrisHCl, 2 % SDS, 10 % Glycerol, 0.1 % Bromphenolblue, 5 mM β-mercaptoethanol). Whole cell lysates were separated on SDS polyacrylamide gels and electro blotted onto nitrocellulose membranes (Whatman). Membranes were blocked for 1 h in 5% (w/v) non-fat milk in TBS-T (20 mM Tris base, 137 mM sodium chloride, 0.1% Tween 20, pH 7.6). After blocking, the membranes were probed with antibodies against CBP (Cell Signaling), p300 (abcam), H3K27ac (abcam), H3K18ac (active motif), fibronectin (abcam), collagen 1 (abcam), p21 (Cell Signaling) or α-tubulin (abcam). As secondary antibodies, horseradish peroxidase-conjugated goat anti-rabbit or goat anti-mouse antibodies (Jackson ImmunoResearch) were used. Signals were detected using the ECL Western blotting detection reagents (GE Healthcare) and the Alpha Imager Software system (Alpha Innotech).

2.6. RNA sequencing of SF

Total RNA from SF was isolated using the RNeasy Mini Kit (Qiagen). The RNA quality and quantity were evaluated using the Agilent RNA 6000 Nano Kit and the Agilent 2100 Bioanalyzer instrument (Agilent Technologies). Library preparation and RNA sequencing (RNAseq) was performed at the Functional Genomics Center Zurich (FGCZ). Libraries for RNAseq were generated using the Illumina TruSeq Stranded total RNA Sample Preparation Kit. The quality and quantity of the generated libraries was checked using the Agilent 2100 Bioanalyzer instrument and a DNA-specific chip. Libraries were sequenced by Illumina NovaSeq 6000, with single read approaches (100bp).

2.7. Bioinformatics analysis of RNA sequencing data

To investigate RNAseq data, we conducted quality control (QC) using *FASTQC* [25], available online at: http://www.bioinformatics.babraham.ac.uk/projects/fastqc. Reads of high quality were mapped to the human reference genome (hg19) using *STAR* [26]. We assessed counts per gene using Feature Counts [27]. We investigated differentially expressed genes (DEG) between experimental conditions using "DESeq2" package of Bioconductor. We removed genes present having less than one count and normalized the remaining counts using Variance Stabilizing Transformation (vsd) approach. We applied Wald test to assess differences between conditions. We set $p \leq 0.05$ after false discovery rate (FDR) adjustment as significant and annotated results using "annotables" package of Bioconductor. For the significantly DEG, we conducted pathway analysis using Gene Ontology (GO) terms and the "clusterProfiler" package of Bioconductor.

For the RNAseq and ChIPseq data integration (see below), we re-run the DEG analysis in the "Limma" model using the "edgeR" package of Bioconductor. This was needed, as BETA software required this format.

2.8. Integration of RNAseq and ChIPseq data

ChIPseq data sets for H3K27ac in RA SF ($n = 3$) were generated previously [22]. H3K27ac peaks were annotated to nearest genes (TSS $\pm$ 3 kb) and genomic features (5 kb flanking regions) using default settings in ChIPseeker package of Bioconductor [28]. We investigated RNAseq and ChIPseq integration in the following steps: 1) overlap, 2) association, and 3) integrative analysis. For step 1), we assessed the overlap between significant DEG (FDR $p < 0.05$, $\pm$ fold change > 1.5) and ChIPseq peaks using Venn diagrams from the "Vennerable" package of R. To assess the number of chromosomal intersections between RNAseq genes and peaks, we applied the "intersect" command from *Bedtools* [29]. In step 2), we investigated associations between ChIPseq peaks in our samples and features in the references genome using the CEAS tool from *Galaxy* [30]. Spearman correlation between bam files was assessed using *DeepTools* [31]. In step 3), we predicted possible activating or repressive functions using the *BETA* (Binding and Expression Target Analysis) software package using 100 kb distance [32].

2.9. ELISA

IL6, IL8 (both BD Biosciences), MMP1, CXCL12, CX3CL1, CCL2, and CCL5 (all R&D Systems) were measured in cell culture supernatants using ELISA according to the manufacturer's instructions.

2.10. Analysis of cell death

Cell viability of transfected SF (5000 cells/well) was analyzed in triplicates using the CytoTox-Glo cytotoxicity assay (Promega) and the Glomax Multi Detection System (Promega).

2.11. Adhesion and proliferation assay

Proliferation and adhesion (towards plastic) of transfected SF was analyzed using an impedance-based system for real-time proliferation and adhesion assays (xCELLigence System, Bucher Biotec AG). Cells were seeded into E-plates 24 h after transfection at a densitiy of 2500 cells/well. TNF (10 ng/ml) was added simultaneously during seeding. Each condition was analyzed in quadruplicates. Impedance changes were recorded every 15 min (0–24 h) and every 30 min (24–120 h). Adhesion was analyzed over the first 2 h of the experiment. Since adhesion was different between conditions, proliferation data were normalized at 30 h, when SF started to proliferate after seeding. Proliferation was analyzed over time (30–120 h).

2.12. Statistical analysis

Statistical analysis on data sets was carried out by using the GraphPad Prism program (GraphPad Software, San Diego, CA). N numbers in all experiments represent biological samples from different patients. Differences between experimental groups were analyzed by analysis of variance (ANOVA) followed by Tukey's multiple comparison test. Data that were not normally distributed, were analyzed by Friedmann test followed by the post hoc Dunn's multiple comparison test. Data are reported as means $\pm$ standard deviations. P values < 0.05 were considered significant.

3. Results

3.1. p300 is the major writer of H3K27ac marks in SF

To study their individual functions, we silenced CBP or p300 in SF in presence and absence of TNF, followed by RNAseq. Silencing was verified by Real-time PCR (Fig. 1A and B) and Western blotting (Fig. 1C). Principal component analysis of RNAseq data showed a clear separation of unstimulated and TNF-stimulated SF (PC1) and revealed a separation of SF silenced for p300 (PC2) from SF silenced for CBP and control SF, which clustered together (Fig. 1E). In line with this, silencing of p300 affected more than five-fold more genes in unstimulated SF, and three-fold more genes in TNF-stimulated SF compared to SF silenced for CBP (Fig. 1F and G). Among the overlapping target genes, 8.1 % in unstimulated SF and 9.0 % in TNF-stimulated SF were regulated in opposite directions by CBP and p300, indicating individual functions of the two enzymes in a subset of overlapping target genes (Supplementary Fig. 2).

The presence of TNF increased the levels of H3K27ac by 92 % ($\pm$39.2 %, $p < 0.05$), indicating substantial *de novo* writing of this activating histone mark in inflammatory conditions. Silencing of p300 had a major impact on the levels of H3K27ac, which was decreased by 32.7 % ($\pm$32.7 %, $p < 0.05$) and 61.1 % ($\pm$21.9 %, $p < 0.05$) in absence and presence of TNF, respectively. In contrast, silencing of CBP only slightly reduced the levels of H3K27ac by 11.3 % ($\pm$46.2 %, n.s.) and 41.2 % ($\pm$34.3 %, n.s.) in absence and presence of TNF (Fig. 1C and D). In addition, we detected a decrease of H3K18ac marks, which was also more pronounced after silencing of p300 compared to silencing of CBP (Suppl. Fig. 1 A, B).

To address the relationship between CBP, p300 and H3K27ac in more detail, we took advantage of our previously generated ChIPseq data set of H3K27ac marks in unstimulated RA SF ($n = 3$) [22]. The majority of H3K27ac marks in SF appeared in distal intergenic and intronic regions of the genome and only 8 % of H3K27ac peaks were found in a 3 kb range of gene promoters, in line with the presence of H3K27ac in promoter and enhancer regions [10]. Within promoter regions, H3K27ac marks were more frequent in proximal compared to distal regions (Fig. 1J). We integrated the H3K27ac peaks with our list of CBP and p300 target genes. First, we assessed the overlap between CBP or p300 target genes with H3K27ac peaks of RA SF. 91.7 % of the CBP target genes and 88,5 % of p300 target genes possessed H3K27ac marks in their promoter or gene flanking regions, which accounted for 5 % and 26 %, respectively, of the overall detected H3K27ac peaks in RA SF (Fig. 1H and I). Next, we integrated RNAseq data with H3K27ac ChIPseq data using BETA, enabling us to analyze the impact of far distant H3K27ac peaks on global CBP and p300 target gene expression. H3K27ac peaks were significantly enriched in genomic regions of >50 kb distances from TSS (data not shown, $p = 1.04 \times 10^{-7}$), and became more enriched at distances of 100 kb from TSS of down regulated genes ($p = 5.61 \times 10^{-7}$), but not of up regulated genes after silencing of p300. Such an association was not found for CBP target genes (Fig. 1K and L). These data suggest that p300 promotes gene expression at far distant enhancers.

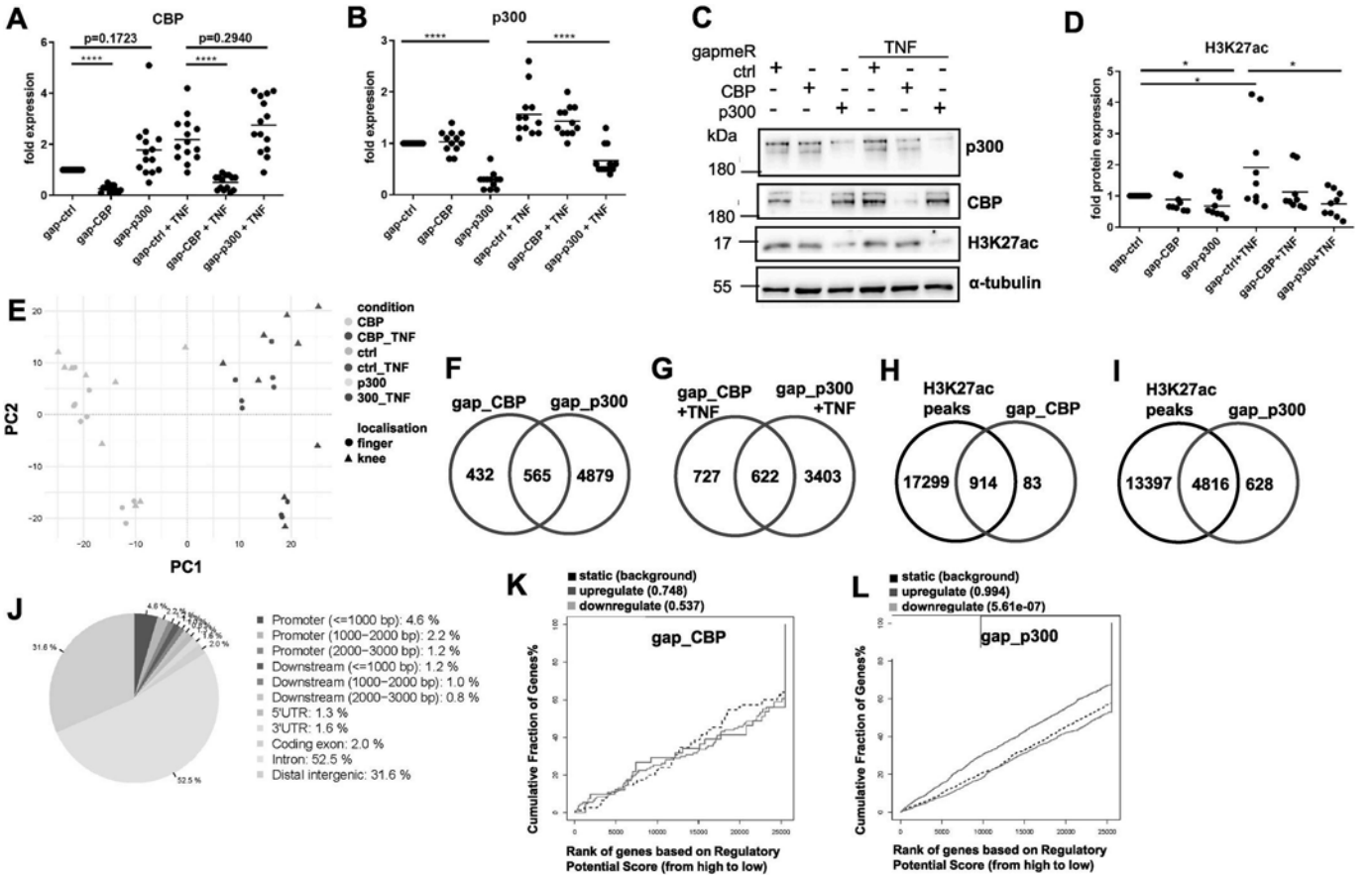

Fig. 1. Silencing of CBP and p300 effects global levels of H3K27ac and expression profiles of SF. CBP and p300 were silenced in SF in absence and presence of TNF (10 ng/ml, 24 h). Silencing of **A.** CBP and **B.** p300 was confirmed by Real time PCR and **C.** by Western blotting. Global levels of H3K27ac were analyzed by Western blotting using the expression of α-tubulin as an endogenous control. Representative Western blots are shown. **D.** Densitometric analysis of Western blots for H3K27ac. **E.** Principal component analysis of RNAseq data using samples from six different independent biological replicates. Triangles indicate SF derived from knee (n = 3), dots indicated SF derived from hand (n = 3). Venn diagrams indicating the number of genes regulated by CBP and p300 in **F.** unstimulated and **G.** TNF-stimulated SF. H3K27ac peaks annotated to **H.** CBP and **I.** p300 target genes in SF. **J.** Proportion of genomic regions enriched for H3K27ac marks in unstimulated SF (n = 3). **K.** and **L.** Integrative analysis of RNAseq and H3K27ac ChIPseq data sets using *BETA* (Binding and Expression Target Analysis). *p < 0.05, ***p < 0.005.

3.2. Identification of pathways regulated by CBP and p300 in SF

To explore which pathways were specifically regulated by CBP or p300, we conducted a pathway analysis of RNAseq data. In unstimulated SF, CBP and p300 regulated core functions of SF, such as "extracellular matrix organization", "DNA replication" and "cell cycle checkpoint" (Suppl. Table 2, Fig. 2A and B). In all three pathways, p300 regulated the majority of target genes, with 18.6 %–29.8 % of p300 target genes being co-regulated by CBP (Fig. 2C). Among the CBP target genes, 25 %–33.3 % were specific for CBP and not co-regulated by p300, underscoring the individual functions of these enzymes in maintaining basic functions of SF on gene levels. Whereas the main function of CBP was associated with all aspects of cell division, p300 silencing additionally affected more diverse pathways, such as "regulation of RNA stability", "ncRNA processing", "organ morphogenesis", "limb development", "WNT signaling" and "cell-substrate adhesion" (Suppl. Table 2, Fig. 2A and B).

In TNF-stimulated SF, we additionally identified several pathways specific for either CBP or p300 silencing (Supplementary Table 2, Fig. 3D and E). This analysis pointed to CBP as the major regulator of inflammatory pathways associated with "interferons", "response to virus", "NF-kappaB signaling" and "cell chemotaxis". The variety of pathways regulated by p300 was extensive, and included genes enriched in "developmental pathways", "differentiation of osteoblasts and chondrocytes", pathways associated with "adhesion", "post-translational protein modification" and the "TNF-mediated signaling pathway". To study the function of CBP and p300 in more detail, we selected some of these pathways for confirmatory studies.

3.3. p300 regulates genes associated with limb development and the positional identity of SF

Developmental pathways are recognized as key pathways activated in RA SF [22,33,34]. We identified enrichment of p300, but no CBP target genes in the biological process (BP) "limb development" (Supplementary Table 2, Fig. 3A). Consistent with our RNAseq data, we confirmed an increased expression of NOTCH1, WNT3 and WNT9a after silencing of p300 (Fig. 3B). We have previously shown that the joint-specific expression of transcripts in the 5′ end of the homeobox (HOX) HOXA and HOXD cluster in peripheral joints is determined by the chromatin landscape [22]. We now analyzed the role of CBP and p300 in the context of this joint-specific expression of HOX genes in SF from hands. In line with their joint-specific expression, the levels of H3K27ac in 5′ regions of the HOXA and the HOXD cluster were enriched in hand SF compared to SF from other joint locations (Fig. 3E and F). Silencing of CBP decreased the expression of HOXA13 and HOXD10. Silencing of p300 increased the expression of HOXA9 and HOXA11, but decreased the expression of HOXA13, HOXD10 and HOXD11 (Fig. 3C and D). Together these data indicate a key role of p300 in developmental pathways in SF and a minor role of CBP in maintaining the joint-specific expression of 5′end HOXA and HOXD transcripts.

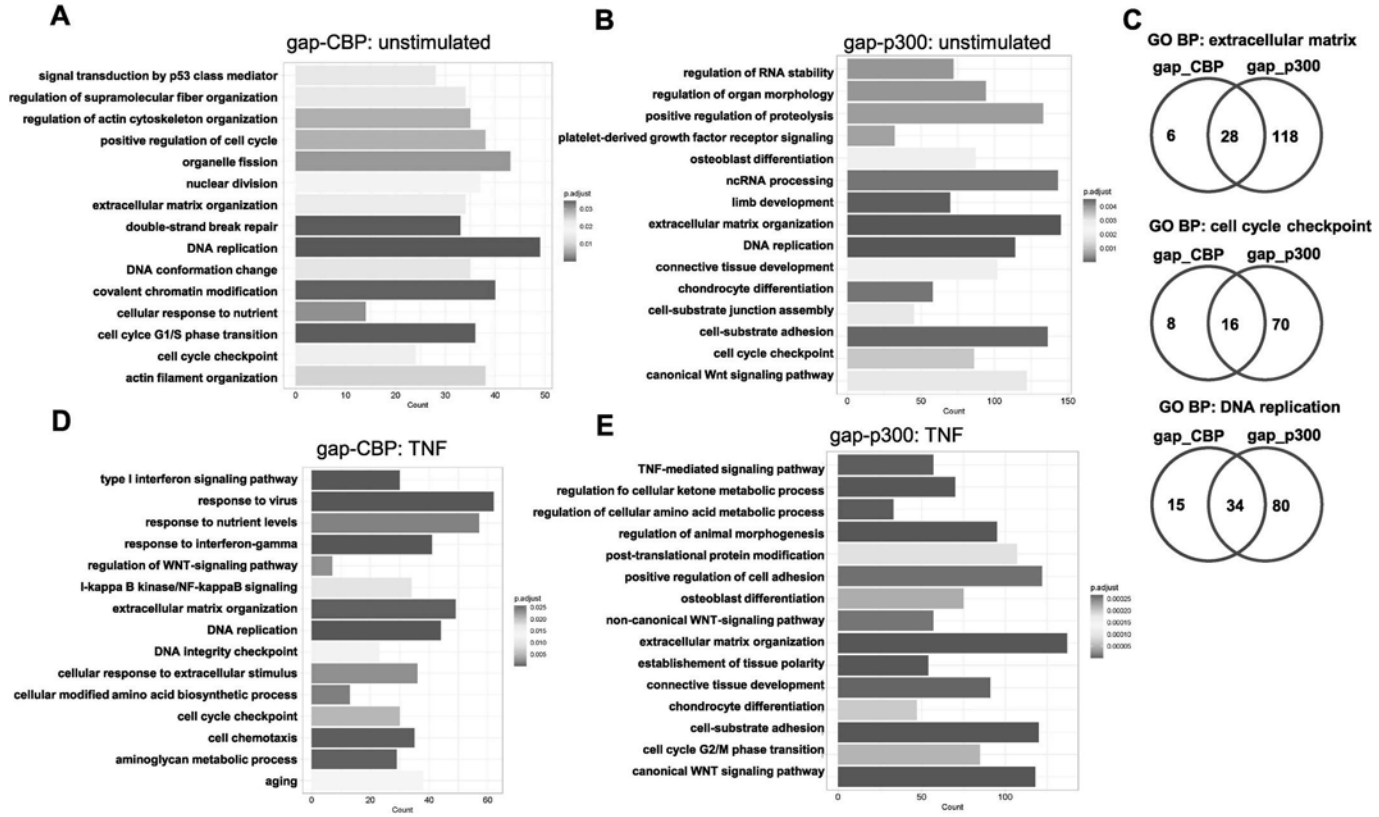

Fig. 2. Pathway enrichment analysis of CBP and p300 target genes. Transcriptomes were determined by RNAseq. Significantly affected genes (±fold change > 1.5, FDR <0.05) entered pathway enrichment analysis for Gene Ontology (GO) biological process (BP) in the "clusterProfiler" package of Bioconductor. Enriched GO BP identified after silencing of **A.** CBP and **B.** p300 in absence and **D.** and **E.** presence of TNF. Displayed pathways were selected from supplementary table 2. **C.** Venn diagrams indicating the proportion of target genes regulated by CBP and p300 in pathways that were overlapping in A. and B.

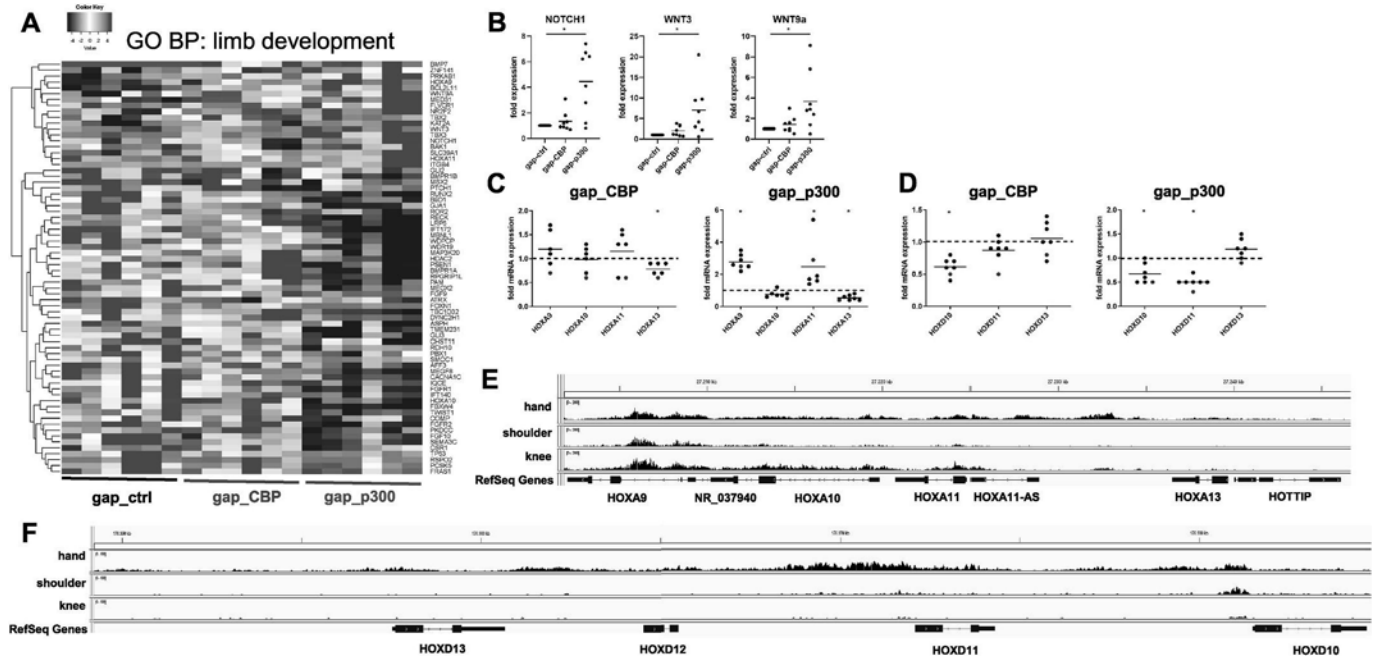

Fig. 3. CBP and p300 regulate developmental pathways in SF. A. Heatmap of DEG (±fold change > 1.5, FDR <0.05) enriched in the biological process (BP) "limb development" that were identified by RNAseq of SF silenced for CBP or p300. **B**. Changes in mRNA expression of selected DEG was analyzed by Real-time PCR in an independent cohort from data shown in A (n = 8). The mRNA expression of genes in the 5′end of the **C.** HOXA and **D.** the HOXD cluster were analyzed by Real-time PCR in RA (black) and OA (red) SF from hand (n = 7). ChIPseq analysis of H3K27ac marks in the **E**. *HOXA* locus and **F**. *HOXD* locus in SF from hand, shoulder and knee.

3.4. CBP and p300 mediate extracellular matrix organization and remodeling

Synthesis of extracellular matrix is a core function of SF [2]. Both in unstimulated and in TNF-stimulated SF, the BP "extracellular matrix organization" was among the top enriched pathways regulated by CBP and p300 (Fig. 2, Suppl. Table 2). This pathway partially overlapped with genes associated with "adhesion" and was composed of genes encoding extracellular matrix proteins, including collagens (COL), fibronectin (FN), and integrins (ITG), matrix-interacting proteins, such as thrombospondins (THBS), and matrix-remodeling enzymes, such as matrix-metalloproteinases (MMP) and ADAM metallopeptidases (Fig. 4A). We validated our findings from RNAseq on mRNA (Fig. 4B) and protein levels (Fig. 4C–F) in an independent sample set derived from RA and OA SF (Supplementary Fig. 3 A). Whereas the global analysis of the pathway "extracellular matrix organization" suggested that p300 is the major enzyme regulating this pathway (Fig. 4A), looking at individual gene levels revealed overlapping and individual functions for CBP and p300. Whereas silencing of CBP down regulated the expression of THBS2 and COL6A3 more pronounced, the suppressive effect of silencing of p300 on THBS1, COL3A1, VCAM1, ADAMTS5 mRNA and FN1 and COL1 protein expression exceeded those of silencing of CBP (Fig. 4B, D-F). We observed the biggest differences in the roles of CBP and p300 regarding the regulation of MMP expression and secretion; silencing of p300 increased the basal and TNF-induced MMP expression and basal MMP1 secretion, whereas silencing of CBP suppressed the TNF-induced MMP expression and MMP1 secretion (Fig. 4B and C).

3.5. CBP and p300 regulate proliferation and adhesion in SF

Given the enrichment of pathways associated with "adhesion" and "cell cycle" and to test whether DEG translate into functional changes of SF, we analyzed SF adhesion and proliferation. In line with our pathways analysis of DEG, silencing of CBP and p300 down regulated SF adhesion in absence and presence of TNF (Fig. 5A and B). Since both factors affected adhesion, we normalized proliferation slopes to 30 h, the time point when control cells started to proliferate after seeding. Both, silencing of CBP and p300 decreased the proliferation of SF in absence and presence of TNF (Fig. 5C and D).

The expression of p21, a potent inhibitor of cell cycle dependent kinases, was increased in SF upon silencing of p300 in absence and presence of TNF, but was not affected upon silencing of CBP (Fig. 5E and F). Cell death was slightly increased in p300 silenced SF in presence of TNF (Fig. 5G), and could therefore not account for the reduced impedance measurements in all other conditions compared to control SF.

3.6. CBP and p300 regulate the inflammatory response of SF

Consistent with our data from RNAseq, silencing of CBP specifically downregulated the expression of genes that were enriched in the pathways "type I interferon signaling pathway" (2′-5′-Oligoadenylate Synthetase 1, OAS1; Signal transducer and activator of transcription 1, STAT1), "response to interferon-γ" (OAS1, STAT1) and "response to virus" (STAT1, IL6, OAS1, CXCL10, CXCL12) (Supplementary Table 2, Fig. 6A). STAT1 is a master transcription factor implicated in regulating TNF-induced interferon response genes in SF (Fig. 6A) [35]. In line with the changes on mRNA levels, the secretion of CXCL12 and IL6 was

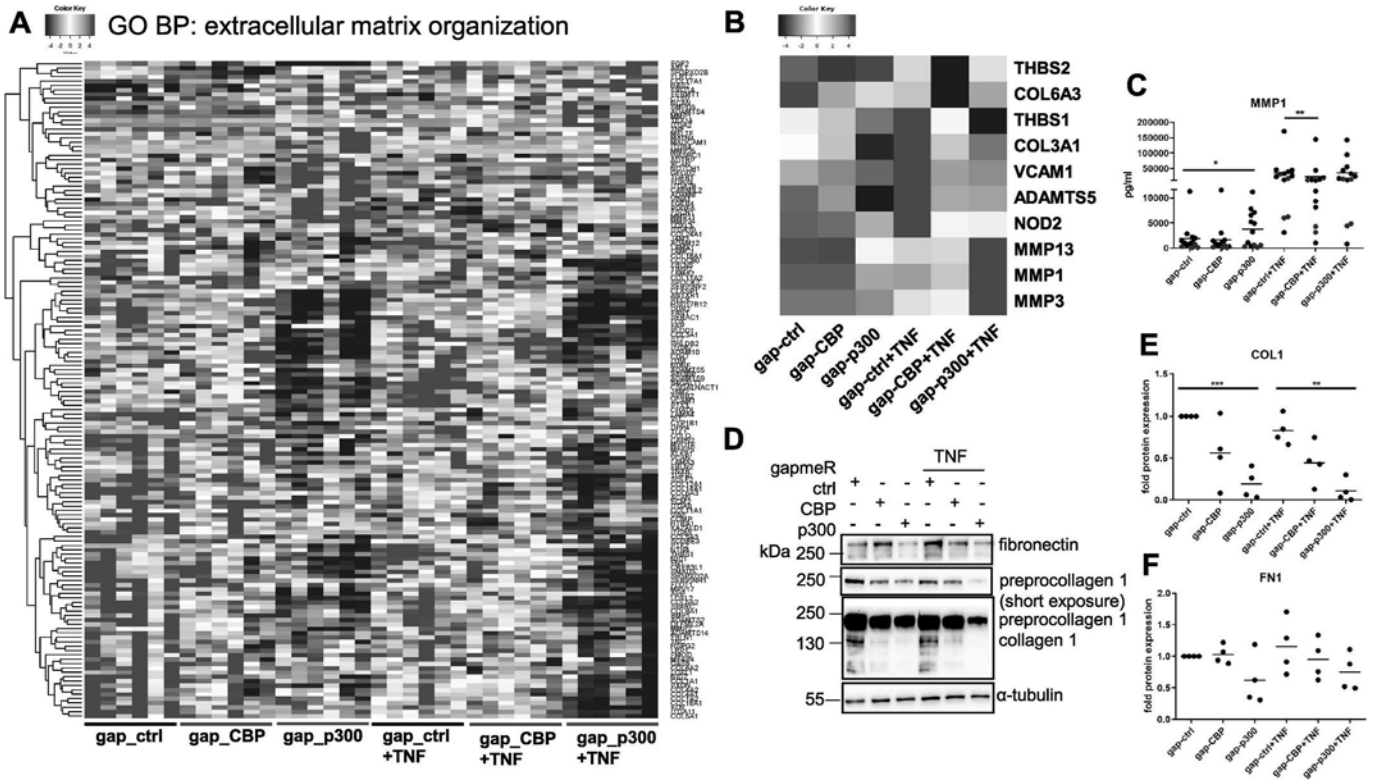

Fig. 4. CBP and p300 regulate the extracellular matrix organization in SF. A. Heatmap of DEG (±fold change > 1.5, FDR <0.05) enriched in the biological process (BP) "extracellular matrix organization" that were identified by RNAseq of SF silenced for CBP or p300 in absence and presence of TNF (10 ng/ml). **B.** Changes in mRNA expression of selected DEG was analyzed by Real-time PCR in an independent cohort from data shown in A. Heatmap shows mean values of fold expression calculated relative to gap-ctrl based on 9–13 independent experiments. **C.** The secretion of MMP1 was analyzed in cell culture supernatants from RA (black) and OA (red) SF (n = 9) silenced for CBP or p300 in absence and presence of TNF (10 ng/ml). **D.** Representative Western blots showing the protein expression of fibronectin (FN1), collagen 1 (COL1) and the house keeping protein α-tubulin in SF silenced for CBP and p300 in absence and presence of TNF (10 ng/ml). **E.** and **F.** Densitometric analysis of D. *p < 0.05, **p < 0.01, ***p < 0.005.

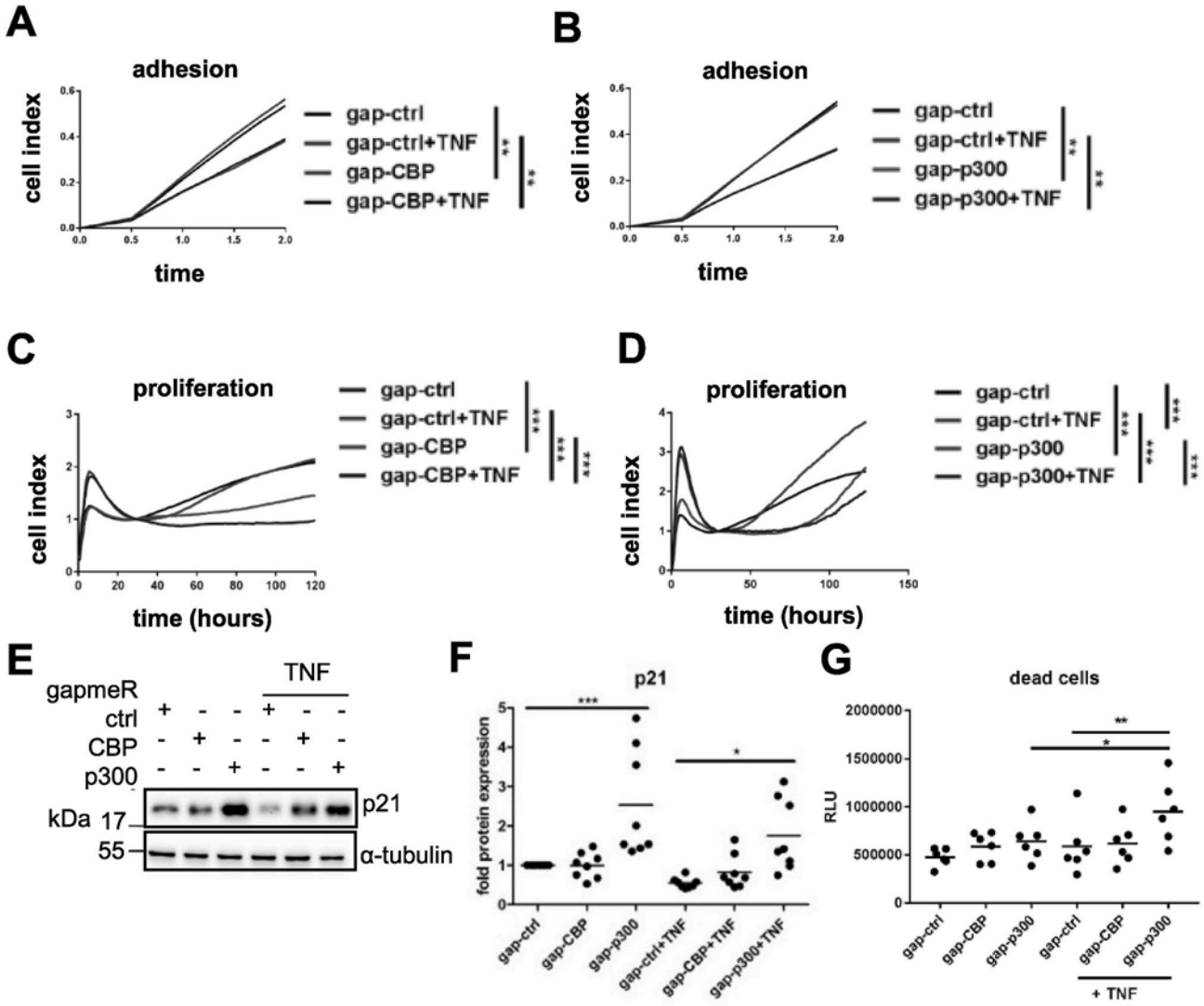

Fig. 5. Silencing of CBP and p300 co-regulate adhesion and proliferation of SF. A. and **B.** adhesion and **C.** and **D.** proliferation of SF (n = 3) after silencing of CBP and p300 in absence and presence of TNF (10 ng/ml) was analyzed using real-time cell-based adhesion and proliferation assays (xCelligence System). **E.** The expression of p21 was analyzed by Western blotting, followed by **F.** densitometric analysis. **G.** Dead cells were evaluated using the CytoTox-Glo cytotoxicity assay (n = 6). *p < 0.05, **p < 0.01.

decreased after silencing of CBP (Fig. 6B).

Given the potential use of CBP/p300 inhibitors as anti-inflammatory drugs, we further analyzed the expression of TNF-induced cytokines and chemokines that we identified to be significantly changed after silencing of CBP and/or p300 in our RNAseq data set (Supplementary Fig. 4). Silencing of CBP resulted in anti-inflammatory effects, indicated by reduction of the TNF-induced gene expression of IL15, CX3CL1, CCL2, IL8 and CCL20, and the decreased secretion of CX3CL1 and CCL5 protein (Fig. 6C and D). In contrast, we detected pro-inflammatory (CXCL2, IL8, CCL20) and anti-inflammatory effects (reduction of IL15, CX3CL1, CCL2, CCL5) after silencing of p300 in presence of TNF (Fig. 6C, D). Effects of CBP and p300 silencing on the inflammatory response was similar in RA and OA SF for all genes analyzed (Suppl. Fig. 3B).

To test potential effects of CBP/p300 inhibitors, we treated SF with TNF in absence and presence of the HAT inhibitor C646 and the bromodomain inhibitor I-CBP, respectively. Both inhibitors reduced the TNF-induced levels of H3K27ac in SF (Fig. 6E and F), indicating that both functional activities, the HAT and the reader (bromo-) domain of CBP/p300 were required for the writing of H3K27ac marks in inflammatory conditions. Treatment with C646 decreased the TNF-induced expression of VCAM1, CX3CL1, IL15, IL8, IL6, MMP1, STAT1, OAS1, CXCL10 and CXCL2 and thus, mirrored with the exception of CXCL2, the effects of CBP silencing. Treatment with I-CBP decreased the TNF-induced expression of genes that were either decreased by both CBP and p300 silencing (NOD2, CCL2, CXCL12, VCAM1, CX3CL1, IL15), or that were decreased by silencing of CBP and not affected by p300 silencing (STAT1, CXCL10). In contrast, genes that were downregulated by silencing of CBP, but increased by silencing of p300, such as OAS1, IL8, MMP1, IL6 and CXCL2 exhibited an increased TNF-induced expression after treatment of I-CBP, indicating that I-CBP-induced effects rather mirrored those obtained by silencing of p300 than by silencing of CBP.

4. Discussion

In this study we have identified p300 as the major HAT that writes H3K27ac marks in SF. H3K27ac marks are activating histone marks present in promoters and enhancers [9]. In unstimulated cells, enhancers and in particular super-enhancers that are marked by the presence of H3K27ac, control and define cell identity [36]. In line with this definition, we showed that the majority of H3K27ac in unstimulated SF was located in distal intergenic and intronic chromatin regions, and

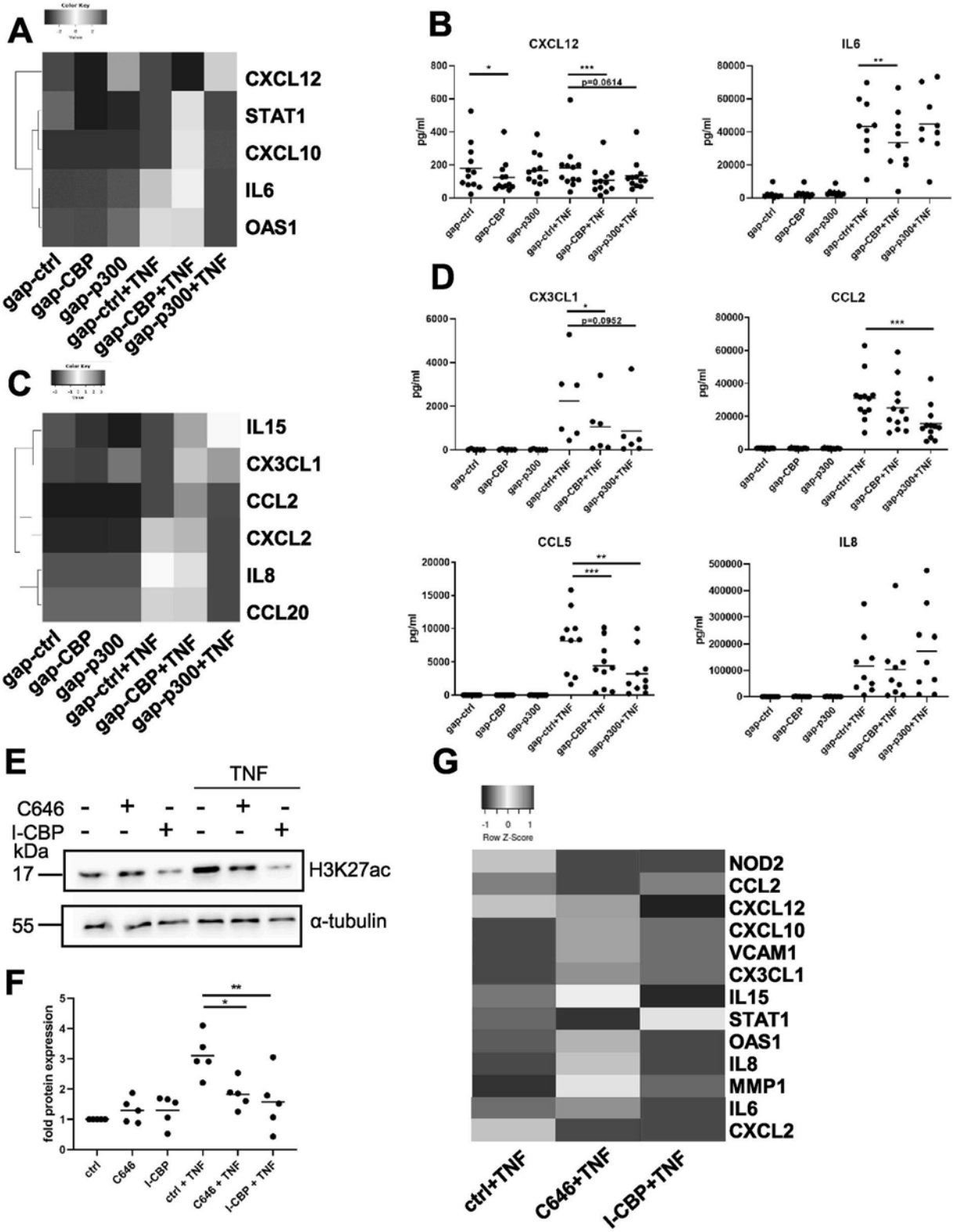

Fig. 6. CBP and p300 regulate the inflammatory response of SF. Heatmaps of selected genes enriched in **A.** "interferon-response and –signaling", and "response to virus" and **C.** genes encoding other cytokines and chemokines verified by Real-time PCR in an independent cohort of SF after silencing of CBP and p300 in absence and presence of TNF. Mean values of fold expression calculated relative to gap-ctrl are shown (n = 13). **B.** and **D.** The secretion of cytokines and chemokines into cell culture supernatants was verified by ELISA. **E.** The levels of H3K27ac in SF treated with C646 or I-CBP were analyzed by Western blotting using the expression of α-tubulin as an endogenous control. Representative Western blots are shown. **F.** densitometric analysis. **G.** Heatmap of selected inflammatory genes verified by Real-time PCR of SF treated with C646 or I-CBP in presence of TNF. Mean values of fold expression calculated relative to unstimulated SF are shown (n = 9–13). *$p < 0.05$, **$p < 0.01$, ***$p < 0.005$.

only a small amount of CBP and p300 target genes exhibited H3K27ac marks in promotors and untranslated gene regions. By silencing of either CBP or p300 in unstimulated SF, we verified that CBP and p300 affected core functions and pathways of SF. In a previous study addressing individual functions of CBP and p300 in primary human myoblasts the authors concluded, that CBP and p300 controlled complementary sets of genes in the same processes [19]. Our findings support a similar conclusion regarding the roles of CBP and p300 in SF. Many of the pathways we identified in SF were co-regulated by CBP and p300, however, both HATs regulated only a subset of overlapping genes and in addition exhibited individual functions on target gene levels. In contrast to the previous study [19], the pathways and target genes regulated by p300 in SF exceeded those regulated by CBP by far, in line with the more pronounced effect of p300 silencing on global levels of H3K27ac.

One of the pathways that was specifically regulated by p300 in SF was "limb development". The crucial role of CBP and p300 in regulating developmental pathways is well established and is underscored by the death of mice carrying a homozygous deletion of either CBP or p300 at early stages of their embryonic development [15]. Several studies have highlighted the role of developmental pathways, including Hox, Notch and Wnt signaling pathways, in RA and in SF biology [22,33,34]. We have previously shown that the expression of HOX transcription factors, that determine the embryonic limb development, is maintained in SF along the proximal-distal and anterior-posterior body axes and might determine the positional disease pattern [22]. Mutations in CBP and p300 lead to the Rubinstein-Taybi syndrome, a rare genetic disorder that is characterized by growth retardation, microcephaly, dysmorphic facial features, and broad thumbs and big toes [37]. The same syndrome was caused by a genetic deletion of a region encompassing *HOXD13*, which is differentially expressed in joints of hand and feet along the anterior-posterior axes [38], and regulatory elements of this cluster [39]. Our data, together with previous findings, indicate that CBP and p300 do not only serve as cofactors for HOX transcription factors [40,41] but overtake individual functions in regulating their expression. CBP/p300 have previously been shown to regulate developmental pathways, including components of the Notch and Wnt signaling pathways, in double knock out mouse embryonic fibroblasts [42]. The Wnt signaling pathway is a main determinant of the bone metabolism in arthritis [34]. The Notch signaling pathway has recently been linked to the differentiation of perivascular and sublining SF [33], and inhibition of Notch1 suppressed the progression of arthritis *in vivo* [43]. Our data point to a major role of p300 and not CBP in regulating these developmental pathways in SF.

Individual functions of CBP and p300 have also been addressed following a different approach in quiescent glioblastoma cells, in which the binding of CBP and p300 to the chromatin strongly overlapped in a 1 kb region up- and downstream of gene bodies. Although there was a high overlap in CBP- and p300-regulated pathways, significant differences in levels of CBP and p300 binding to the chromatin, as well as potential differences in interactions with transcription factors have been detected [18]. Results solely based on the recruitment of HATs to chromatin have to be handled with care, since recruitment of CBP to chromatin regions was not sufficient to predict effects on gene expression of nearby genes in mouse embryonic fibroblasts [44]. 45 % of CBP peaks identified in this study by ChIPseq were detected in chromatin regions of more than 50 kb distance to known gene promoters [44], a finding that strongly resemble the results of our integrative analysis of p300 RNAseq and H3K27ac ChIPseq data sets. We did not detect such an association between H3K27ac marks and CBP target genes. This might be related to the lower number of CBP target genes identified. Another possibility is the involvement of other molecular mechanisms beyond the acetylation of H3K27, e.g. acetylation of H3K18 or H2B, that might direct CBP-dependent gene regulation [12,42]. In line with these previous reports, we showed that silencing of CBP and p300 did not only decrease global levels of H3K27ac but also affected levels of H3K18ac in SF.

Our integrative analysis of RNAseq and ChIPseq data could not explain the upregulation of genes upon p300 silencing. Although H3K27ac is in general considered as an activating histone mark [9], a p300-dependent repression of transcription has been described earlier [45]. Another explanation for the increased gene expression upon silencing of the two HATs might be the involvement of differential acetylation of non-histone proteins. A study in mouse embryonic fibroblasts estimated that CBP/p300 function accounted for up to one third of the nuclear acetylome [42].

Chromatin remodeling is a key event in the inflammatory response of SF [7,8,46]. In line with a previous study, differences in CBP and p300 functions became more apparent after stimulation [18]. We showed that stimulation of SF with TNF led to a substantial *de novo* writing of H3K27ac, indicating that the inflammatory response of SF is not solely based on a re-distribution of enhancers. *Loh* et *al.* showed that the persistence of the TNF-induced H3K27ac in a ±2 kb region around the transcription start site was associated with a sustained expression of pro-inflammatory genes in SF. In particular, gene clusters associated with a long-lasting H3K27ac in their promoter and proximal enhancer regions encoded for cytokines and chemokines [8]. This mechanism provided a potential link between the inflammatory gene expression in SF and the chronic unremitting synovitis in RA. Previous studies, comparing DNA methylation signatures in early, resolving and established RA, have indicated that some epigenetic changes occur early in disease [47,48]. Among the identified pathways regulated in early and established RA that were absent in resolving RA, were integrin, cadherin and WNT cell adhesion signaling pathways, components of the actin cytoskeleton and antigen presentation [48]. Some of these pathways were also enriched in our pathway analysis, suggesting that CBP and/or p300 could potentially contribute to reported functional changes of SF in early RA [49]. However, to prove this, further studies in samples from different disease stages would be needed. Our study was based largely on SF derived from established RA. A comparison of effects of CBP and p300 silencing in a small number of OA SF has revealed similar effects in RA and OA SF.

Silencing of CBP induced anti-inflammatory effects, and specifically down regulated genes associated with an interferon signature. Type I interferon signature genes were shown to be associated with disease activity in RA and predicted clinical outcome [50]. Silencing of p300 provoked several pro-inflammatory and pro-destructive effects, indicated by an increased expression of NOTCH1, MMPs and cytokines and chemokines. Based on our data obtained by the use of I-CBP we suggest an involvement of the bromodomain of p300 in this mechanism. In contrast, C646 treatment did not mirror p300 silencing-induced gene expression, suggesting that HAT domain and H3K27ac were not involved in the increase of gene expression. These data again confirmed our integrative analysis of RNAseq and ChIPseq analysis that detected an association of down regulated but not up regulated genes after p300 silencing. Data sets obtained by the use of inhibitors did not fully overlap with results obtained by silencing. These differences might be explained by either blocking a sole domain by inhibitor treatment, in contrast to disrupting protein-protein interactions by removing an entire protein that serves as scaffolding platform for several proteins by the silencing approach. The molecular basis underlying different functions of CBP and p300, and the effects of different inhibitors mirroring more the effects of p300 than of CBP, is largely obscure. A comparative mutational analysis of the HAT domains of the CBP and p300 revealed some structural differences that might underlie individual functions, despite their high degree of sequence homology. Whereas the PHD finger of p300 was shown to be dispensable for its HAT activity, it was essential for CBP. Furthermore, identical mutations impaired HAT activities of CBP and p300 differentially [51].

5. Conclusion

We provide new mechanistic insights in how CBP and p300 regulate the constitutive and inflammatory response of SF and have identified

p300 as the major HAT in SF. Whereas silencing of CBP induced anti-inflammatory effects, silencing of p300 provoked pro- and anti-inflammatory effects. Inhibitor treatment of SF resembled to a large extent effects of p300 silencing, indicating that CBP/p300 inhibitors are not sufficient to control the inflammatory response of SF.

Funding

This work was supported by the Swiss National Foundation (PMPDP3-171,315) and the Foundation for Research in Science and the Humanities at the University of Zurich (STWF-10-004). MK received a scientific training bursary provided by EULAR.

Acknowledgements

We thank Maria Comazzi and Peter Künzler for excellent technical assistance.

Appendix A. Supplementary data

Supplementary data to this article can be found online at https://doi.org/10.1016/j.jaut.2021.102709.

References

[1] J.S. Smolen, D. Aletaha, I.B. McInnes, Rheumatoid arthritis, Lancet 388 (2016) 2023–2038, 10055.
[2] C. Ospelt, Synovial fibroblasts in 2017, RMD Open 3 (2) (2017), e000471.
[3] S. Lefevre, A. Knedla, C. Tennie, A. Kampmann, C. Wunrau, R. Dinser, et al., Synovial fibroblasts spread rheumatoid arthritis to unaffected joints, Nat. Med. 15 (12) (2009) 1414–1420.
[4] B. Zimmermann-Geller, S. Koppert, N. Kesel, R. Hasseli, S. Ullrich, S. Lefevre, et al., Interactions between rheumatoid arthritis synovial fibroblast migration and endothelial cells, Immunol. Cell Biol. 97 (2) (2019) 178–189.
[5] A.P. Croft, J. Campos, K. Jansen, J.D. Turner, J. Marshall, M. Attar, et al., Distinct fibroblast subsets drive inflammation and damage in arthritis, Nature 570 (7760) (2019) 246–251.
[6] F. Zhang, K. Wei, K. Slowikowski, C.Y. Fonseka, D.A. Rao, S. Kelly, et al., Defining inflammatory cell states in rheumatoid arthritis joint synovial tissues by integrating single-cell transcriptomics and mass cytometry, Nat. Immunol. (2019).
[7] K. Klein, M. Frank-Bertoncelj, E. Karouzakis, R.E. Gay, C. Kolling, A. Ciurea, et al., The epigenetic architecture at gene promoters determines cell type-specific LPS tolerance, J. Autoimmun. 83 (2017) 122–133.
[8] C. Loh, S.H. Park, A. Lee, R. Yuan, L.B. Ivashkiv, G.D. Kalliolias, TNF-induced inflammatory genes escape repression in fibroblast-like synoviocytes: transcriptomic and epigenomic analysis, Ann. Rheum. Dis. 78 (9) (2019) 1205–1214.
[9] M.P. Creyghton, A.W. Cheng, G.G. Welstead, T. Kooistra, B.W. Carey, E.J. Steine, et al., Histone H3K27ac separates active from poised enhancers and predicts developmental state, Proc. Natl. Acad. Sci. U. S. A. 107 (50) (2010) 21931–21936.
[10] E. Calo, J. Wysocka, Modification of enhancer chromatin: what, how, and why? Mol. Cell. 49 (5) (2013) 825–837.
[11] M. Ding, Y. Liu, X. Liao, H. Zhan, Y. Liu, W. Huang, Enhancer RNAs (eRNAs): new insights into gene transcription and disease treatment, J. Canc. 9 (13) (2018) 2334–2340.
[12] Q. Jin, L.R. Yu, L. Wang, Z. Zhang, L.H. Kasper, J.E. Lee, et al., Distinct roles of GCN5/PCAF-mediated H3K9ac and CBP/p300-mediated H3K18/27ac in nuclear receptor transactivation, EMBO J. 30 (2) (2011) 249–262.
[13] A. Visel, M.J. Blow, Z. Li, T. Zhang, J.A. Akiyama, A. Holt, et al., ChIP-seq accurately predicts tissue-specific activity of enhancers, Nature 457 (7231) (2009) 854–858.
[14] D.C. Bedford, L.H. Kasper, T. Fukuyama, P.K. Brindle, Target gene context influences the transcriptional requirement for the KAT3 family of CBP and p300 histone acetyltransferases, Epigenetics : official journal of the DNA Methylation Society 5 (1) (2010) 9–15.
[15] E. Kalkhoven, CBP and p300: HATs for different occasions, Biochem. Pharmacol. 68 (6) (2004) 1145–1155.
[16] D. Shi, M.S. Pop, R. Kulikov, I.M. Love, A.L. Kung, S.R. Grossman, CBP and p300 are cytoplasmic E4 polyubiquitin ligases for p53, Proc. Natl. Acad. Sci. U. S. A. 106 (38) (2009) 16275–16280.
[17] T.A. Popp, C. Tallant, C. Rogers, O. Fedorov, P.E. Brennan, S. Muller, et al., Development of selective CBP/P300 benzoxazepine bromodomain inhibitors, J. Med. Chem. 59 (19) (2016) 8889–8912.
[18] Y.F. Ramos, M.S. Hestand, M. Verlaan, E. Krabbendam, Y. Ariyurek, M. van Galen, et al., Genome-wide assessment of differential roles for p300 and CBP in transcription regulation, Nucleic Acids Res. 38 (16) (2010) 5396–5408.
[19] L. Fauquier, K. Azzag, M.A.M. Parra, A. Quillien, M. Boulet, S. Diouf, et al., CBP and P300 regulate distinct gene networks required for human primary myoblast differentiation and muscle integrity, Sci. Rep. 8 (1) (2018) 12629.
[20] F.C. Arnett, S.M. Edworthy, D.A. Bloch, D.J. McShane, J.F. Fries, N.S. Cooper, et al., The American Rheumatism Association 1987 revised criteria for the classification of rheumatoid arthritis, Arthritis Rheum. 31 (3) (1988) 315–324.
[21] R. Altman, E. Asch, D. Bloch, G. Bole, D. Borenstein, K. Brandt, et al., Development of criteria for the classification and reporting of osteoarthritis. Classification of osteoarthritis of the knee. Diagnostic and Therapeutic Criteria Committee of the American Rheumatism Association, Arthritis Rheum. 29 (8) (1986) 1039–1049.
[22] M. Frank-Bertoncelj, M. Trenkmann, K. Klein, E. Karouzakis, H. Rehrauer, A. Bratus, et al., Epigenetically-driven anatomical diversity of synovial fibroblasts guides joint-specific fibroblast functions, Nat. Commun. 8 (2017) 14852.
[23] K. Klein, P.A. Kabala, A.M. Grabiec, R.E. Gay, C. Kolling, L.L. Lin, et al., The bromodomain protein inhibitor I-BET151 suppresses expression of inflammatory genes and matrix degrading enzymes in rheumatoid arthritis synovial fibroblasts, Ann. Rheum. Dis. 75 (2) (2016) 422–429.
[24] T.D. Schmittgen, K.J. Livak, Analyzing real-time PCR data by the comparative C(T) method, Nat. Protoc. 3 (6) (2008) 1101–1108.
[25] S.W. Wingett, S. Andrews, FastQ Screen: a tool for multi-genome mapping and quality control. F1000Res 7 (2018) 1338.
[26] A. Dobin, C.A. Davis, F. Schlesinger, J. Drenkow, C. Zaleski, S. Jha, et al., STAR: ultrafast universal RNA-seq aligner, Bioinformatics 29 (1) (2013) 15–21.
[27] Y. Liao, G.K. Smyth, W. Shi, featureCounts: an efficient general purpose program for assigning sequence reads to genomic features, Bioinformatics 30 (7) (2014) 923–930.
[28] G. Yu, L.G. Wang, Q.Y. He, ChIPseeker: an R/Bioconductor package for ChIP peak annotation, comparison and visualization, Bioinformatics 31 (14) (2015) 2382–2383.
[29] A.R. Quinlan, I.M. Hall, BEDTools: a flexible suite of utilities for comparing genomic features, Bioinformatics 26 (6) (2010) 841–842.
[30] E. Afgan, D. Baker, B. Batut, M. van den Beek, D. Bouvier, M. Cech, et al., The Galaxy platform for accessible, reproducible and collaborative biomedical analyses: 2018 update, Nucleic Acids Res. 46 (W1) (2018) W537–W544.
[31] F. Ramirez, F. Dundar, S. Diehl, B.A. Gruning, T. Manke, deepTools: a flexible platform for exploring deep-sequencing data, Nucleic Acids Res. 42 (2014) W187–W191. Web Server issue.
[32] S. Wang, H. Sun, J. Ma, C. Zang, C. Wang, J. Wang, et al., Target analysis by integration of transcriptome and ChIP-seq data with BETA, Nat. Protoc. 8 (12) (2013) 2502–2515.
[33] K. Wei, I. Korsunsky, J.L. Marshall, A. Gao, G.F.M. Watts, T. Major, et al., Notch signalling drives synovial fibroblast identity and arthritis pathology, Nature 582 (7811) (2020) 259–264.
[34] D. Cici, A. Corrado, C. Rotondo, F.P. Cantatore, Wnt signaling and biological therapy in rheumatoid arthritis and spondyloarthritis, Int. J. Mol. Sci. 20 (22) (2019).
[35] B. Burja, T. Mertelj, M. Frank-Bertoncelj, Hi-JAKi-ng synovial fibroblasts in inflammatory arthritis with JAK inhibitors, Front. Med. 7 (2020) 124.
[36] D. Hnisz, B.J. Abraham, T.I. Lee, A. Lau, V. Saint-Andre, A.A. Sigova, et al., Super-enhancers in the control of cell identity and disease, Cell 155 (4) (2013) 934–947.
[37] D. Milani, F.M. Manzoni, L. Pezzani, P. Ajmone, C. Gervasini, F. Menni, et al., Rubinstein-Taybi syndrome: clinical features, genetic basis, diagnosis, and management, Ital. J. Pediatr. 41 (2015) 4.
[38] C. Ospelt, M. Frank-Bertoncelj, Why location matters - site-specific factors in rheumatic diseases, Nat. Rev. Rheumatol. 13 (7) (2017) 433–442.
[39] C. Gervasini, F. Mottadelli, R. Ciccone, P. Castronovo, D. Milani, G. Scarano, et al., High frequency of copy number imbalances in Rubinstein-Taybi patients negative to CREBBP mutational analysis, Eur. J. Hum. Genet. 18 (7) (2010) 768–775.
[40] F. Ladam, C.G. Sagerstrom, Hox regulation of transcription: more complex(es), Dev. Dynam. 243 (1) (2014) 4–15.
[41] M. Camos, J. Esteve, P. Jares, D. Colomer, M. Rozman, N. Villamor, et al., Gene expression profiling of acute myeloid leukemia with translocation t(8;16)(p11;p13) and MYST3-CREBBP rearrangement reveals a distinctive signature with a specific pattern of HOX gene expression, Canc. Res. 66 (14) (2006) 6947–6954.
[42] B.T. Weinert, T. Narita, S. Satpathy, B. Srinivasan, B.K. Hansen, C. Scholz, et al., Time-resolved analysis reveals rapid dynamics and broad scope of the CBP/p300 acetylome, Cell 174 (1) (2018) 231–244 e12.
[43] J.S. Park, S.H. Kim, K. Kim, C.H. Jin, K.Y. Choi, J. Jang, et al., Inhibition of notch signalling ameliorates experimental inflammatory arthritis, Ann. Rheum. Dis. 74 (1) (2015) 267–274.
[44] L.H. Kasper, C. Qu, J.C. Obenauer, D.J. McGoldrick, P.K. Brindle, Genome-wide and single-cell analyses reveal a context dependent relationship between CBP recruitment and gene expression, Nucleic Acids Res. 42 (18) (2014) 11363–11382.
[45] L. Zhao, E.A. Glazov, D.R. Pattabiraman, F. Al-Owaidi, P. Zhang, M.A. Brown, et al., Integrated genome-wide chromatin occupancy and expression analyses identify key myeloid pro-differentiation transcription factors repressed by Myb, Nucleic Acids Res. 39 (11) (2011) 4664–4679.
[46] K. Klein, S. Gay, Epigenetics in rheumatoid arthritis, Curr. Opin. Rheumatol. 27 (1) (2015) 76–82.
[47] R. Ai, J.W. Whitaker, D.L. Boyle, P.P. Tak, D.M. Gerlag, W. Wang, et al., DNA methylome signature in synoviocytes from patients with early rheumatoid arthritis compared to synoviocytes from patients with longstanding rheumatoid arthritis, Arthritis & rheumatology. 67 (7) (2015) 1978–1980.
[48] E. Karouzakis, K. Raza, C. Kolling, C.D. Buckley, S. Gay, A. Filer, et al., Analysis of early changes in DNA methylation in synovial fibroblasts of RA patients before diagnosis, Sci. Rep. 8 (1) (2018) 7370.

[49] A. Filer, L.S.C. Ward, S. Kemble, C.S. Davies, H. Munir, R. Rogers, et al., Identification of a transitional fibroblast function in very early rheumatoid arthritis, Ann. Rheum. Dis. 76 (12) (2017) 2105–2112.
[50] J. Rodriguez-Carrio, M. Alperi-Lopez, P. Lopez, F.J. Ballina-Garcia, A. Suarez, Heterogeneity of the type I interferon signature in rheumatoid arthritis: a potential limitation for its use as a clinical biomarker, Front. Immunol. 8 (2017) 2007.
[51] L. Bordoli, S. Husser, U. Luthi, M. Netsch, H. Osmani, R. Eckner, Functional analysis of the p300 acetyltransferase domain: the PHD finger of p300 but not of CBP is dispensable for enzymatic activity, Nucleic Acids Res. 29 (21) (2001) 4462–4471.